Genomic oropharyngeal Neisseria surveillance detects MALDI-TOF MS species misidentifications and reveals a novel Neisseria cinerea clade Subscribed

Tessa de Block[1], Irith De Baetselier[1], Dorien Van den Bossche[1], Saïd Abdellati[1], Zina Gestels[1], Jolein Gyonne Elise Laumen[1], Christophe Van Dijck[1], Thibaut Vanbaelen[1], Nathalie Claes[2], Koen Vandelannoote[3], Chris Kenyon[1], Odile Harrison[4] and Sheeba Santhini Manoharan-Basil[1]

Affiliations:

[1]Department of Clinical Sciences, Institute of Tropical Medicine, 2000 Antwerp, Belgium

[2]EMAT, University of Antwerp, Groenenborgerlaan 171, 2020 Antwerp, Belgium

[3]Bacterial Phylogenomics group, Institut Pasteur du Cambodge, Phnom Penh, Cambodia

[4]Nuffield Department of Population Health, Infectious Diseases Epidemiology Unit, University of Oxford, Oxford, UK

*Correspondence: Tessa de Block, tdeblock@itg.be

ABSTRACT

Introduction. Commensal Neisseria spp. are highly prevalent in the oropharynx as part of the healthy microbiome. N. meningitidis can colonise the oropharynx too from where it can cause invasive meningococcal disease. To identify N. meningitidis, clinical microbiology laboratories often rely on Matrix Assisted Laser Desorption/Ionisation Time of Flight Mass Spectrometry (MALDI-TOF MS).

Hypothesis/Gap statement. N. meningitidis may be misidentified by MALDI-TOF MS.

Aim. To conduct genomic surveillance of oropharyngeal Neisseria spp. in order to: (i) verify MALDI-TOF MS species identification, and (ii) characterize commensal Neisseria spp. genomes.

Methodology. We analysed whole genome sequence (WGS) data from 119 Neisseria spp. isolates from a surveillance programme for oropharyngeal Neisseria spp. in Belgium. Different species identification methods were compared: (i) MALDI-TOF MS, (ii) Ribosomal Multilocus Sequence Typing (rMLST) and (iii) rplF gene species identification. WGS data were used to further characterize Neisseria species found with supplementary analyses of Neisseria cinerea genomes.

Results. Based on genomic species identification, isolates from the oropharyngeal Neisseria surveilence study were composed of the following species: N. meningitidis (n=23), N. subflava (n=61), N. mucosa (n=15), N. oralis (n=8), N. cinerea (n=5), N. elongata (n=3), N. lactamica (n=2), N. bacilliformis (n=1) and N. polysaccharea (n=1). Of these 119 isolates, four isolates identified as N. meningitidis (n=3) and N. subflava (n=1) by MALDI-TOF MS, were determined to be N. polysaccharea (n=1), N. cinerea (n=2) and N. mucosa (n=1) by rMLST. Phylogenetic analyses revealed that N. cinerea isolates from the general population (n=3, cluster one) were distinct from those obtained from men who have sex with men (MSM, n=2, cluster two). The latter contained genomes misidentified as N. meningitidis using MALDI-TOF MS. These two N. cinerea clusters persisted after the inclusion of published N. cinerea WGS (n=42). Both N. cinerea clusters were further defined through pangenome and Average Nucleotide Identity (ANI) analyses.

Conclusion. This study provides insights into the importance of genomic genus-wide Neisseria surveillance studies to improve the characterization and identification of the Neisseria genus.

Keywords

genome dynamics, genomic surveillance, MALDI-TOF MS, Neisseria cinerea, Neisseria meningitidis, species boundaries, species identification, rMLST

Author Notes

†These authors contributed equally to this work

The genome assemblies from isolates from this study will be openly available at PubMLST.org/neisseria database with unique PubMLST id number as reported in Supplemental Table 1.

Eight supplementary figures and nine supplementary tables are available with the online version of this article.

Abbreviations

ANI, average nucleotide identity; ChewBBACA, blast score ratio based allele calling algorithm; CREE, correia repeat enclosed elements; DUS, DNA uptakesequence; HGT, horizontal gene transfer; ITM, Institute of Tropical Medicine; iTOL, interactive tree of life; MALDI-TOF MS, matrix assisted laser desorption/ionisation time of flight mass spectrometry; MICs, minimum inhibitory concentrations; ML, maximum-likelihood; MLST, multi locus sequence typing; MSM, men who have sex with men; MSQ, mass spectral quality; PrEP, pre-exposure prophylaxis; rMLST, ribosomal multilocus sequence typing; SEM, secondary electron (SE) scanning electron microscopy; WGS, whole genome sequence.

Data Summary

In addition to the 119 isolates studied here, a selection of published Neisseria spp. genome assemblies were included in our analysis to provide appropriate phylogenetic context for interpreting the diversity of commensal Neisseria. This consisted of genome assemblies from the study by [1], a commensal Neisseria WGS study on isolates from MSM cohort in Belgium (PRJNA703317), and a selection of genome assemblies used in the study by [2], a phylogenetic study of global Neisseria spp. to detect HGT of fluoroquinolone resistance-conferring genes. An overview of the study genomes and those from the additional datasets is shown in Table S2. An overview of which genomes were used per analysis is shown in Supplemental Data file – Fig. S1, available in the online version of this article.

Impact Statement

MALDI-TOF MS is a widely used technique to identify bacteria species, but misidentification of Neisseria spp. is reported. Initially, we used MALDI-TOF MS to identify isolates from a oropharyngeal Neisseria spp. surveillance programme in Belgium. After WGS, we used genomic data to validate MALDI-TOF MS results. By doing so, we were able to detect important MALDI-TOF MS species misidentifications, e.g. two N. cinerea isolates were misidentified as N. meningitidis. Moreover, we discovered that N. cinerea is composed of two distinct clusters. Phylogenetic analysis of all available, globally distributed N. cinerea genomes confirmed two different N. cinerea clusters. This study shows that ongoing surveillance of circulating Neisseria spp. that includes WGS is required to adequately characterize commensal and pathogenic Neisseria spp.

Introduction

Commensal Neisseria species form part of the normal human oropharyngeal microbiome. Although they occasionally cause invasive infections in immunocompromised individuals, they play an important role in maintaining a healthy oropharynx through the displacement of resident pathogenic Neisseria spp. as well as the prevention of colonization by pathogenic Neisseria spp. [3–8]. They also provide an important reservoir of genetic material conferring antimicrobial resistance that can be acquired by the pathogenic Neisseria spp., N. gonorrhoeae and N. meningitidis through horizontal gene transfer (HGT) [9–12].

The advent of Whole Genome Sequencing (WGS) has significantly enhanced the accuracy and reliability of Neisseria species identification. A commonly used genomic species identification method, Ribosomal Multilocus Sequence Typing (rMLST), uses the information from 53 genes encoding the bacterial ribosome subunit offering a robust tool for universal species identification [13]. Another genomic approach often used in Neisseria species identification is based on the nucleotide sequence of the rplF gene [14]. Furthermore, genomic data has been used to verify species identification by Matrix Assisted Laser Desorption/Ionisation Time of Flight Mass Spectrometry (MALDI-TOF MS). Several studies have described detailed instances where MALDI-TOF MS misidentified commensal Neisseria spp. as N. meningitidis or vice versa [15–19]. Additionally, the use of WGS in the genomic characterization of Neisseria species has resulted in a number of important consolidated reclassifications: N. subflava biovar subflava, perflava, flava, and flavescens have been combined into N. subflava, and N. sicca and N. mucosa have been merged into N. mucosa [20, 21]. New Neisseria species have been identified based on whole genome data by studying the phylogenetic relatedness of different gene panels and the nucleotide relatedness by average nucleotide identity (ANI) [22, 23].

This manuscript reports the results of a WGS surveillance programme of 119 Neisseria isolates as part of an oropharyngeal Neisseria spp. surveillance study of two distinct Belgian cohorts: men who have sex with men (MSM) and the general population [24]. The MSM cohort is distinguished by elevated levels of antimicrobial and HIV pre-exposure prophylaxis (PrEP) consumption. During the first phase of the surveillance study, identification of oropharyngeal Neisseria species was accomplished using MALDI-TOF MS, and their antimicrobial susceptibilities were assessed [24]. In this second phase of the study, we conducted WGS of the isolates, which revealed errors with MALDI-TOF MS-based species identification. In addition, phylogenetic analyses revealed a novel clade of Neisseria cinerea.

Methods

Sample collection and processing

Neisseria isolates selected for WGS originated from cultures of oropharyngeal swabs (ESwabs COPAN Diagnostics Inc., Italy) from 64 MSM who participated in a mouthwash randomized controlled trial at the Institute of Tropical Medicine (ITM) in Antwerp, Belgium [25]. The swabs were collected prior to the initiation of any other study procedures, including the application of the designated study mouthwash. In addition, oropharyngeal samples were collected from 32 individuals representing the general Belgian population, using identical sampling and culture protocols [24].

Identification of Neisseria spp. using MALDI-TOF Mass Spectrometry

Isolates were cultured by streaking onto BD Columbia Agar plates with 5% sheep blood, followed by incubation at 37°C with 5% CO2. Individual colonies displaying morphology indicative of Neisseria spp. were selected. Species-level identification was carried out using MALDI-TOF MS on a Bruker MALDI

Biotyper Sirius IVD system using the MBT Compass IVD software and library (Bruker Daltonics, Bremen, Germany). As described by [24], a linear mode in a mass range of 2–20 kDa was set to acquire the spectra of the isolates. The N. mucosa category included N. macacae, and the N. subflava category included N. perflava and N. flavescens. The 119 isolates selected for downstream WGS were identified as N. meningitidis (n=26) and commensal Neisseria (n=93). Among the panel of 119 isolates, 61 were derived from participants (n=43) from the MSM cohort, while 58 originated from participants (n=32) from the general Belgian population cohort.

gDNA extraction, whole genome sequencing

Overnight cultures from the selected isolate panel (n=119) were rapidly snap-frozen using liquid nitrogen and outsourced to Eurofins genomics (Konstanz, Germany) for gDNA extraction, followed by library preparation using Illumina TruSeq DNA kit. Whole genome sequencing was carried out on the NovaSeq 6000 platform, (Illumina Inc, San Diego, CA, USA) using 2×150 bp paired-end sequencing chemistry. The quality of the raw reads was assessed using FASTQC [26]. We used trimmomatic (v0.39) [27] to trim residual sequencing adaptors and crop the 3' end of reads where quality monotonically decreases [27].

De novo assembly and MLST genotyping

Processed Illumina reads were de novo assembled with Shovill (v 1.0.4), which uses SPAdes (v 3.14.0), using the following: parameters –depth 150–opts–isolate [28, 29]. Contigs below 500 bp were excluded from further analysis. Assembly quality was verified with QUAST (v 5.0.2) (Table S1) [30]. Annotation was performed by using Prokka (v 1.14.6) [31]. All the de novo assembled genomes were uploaded to the PubMLST.org/neisseria database, which is powered by the genomics software, BIGSdb, and each record possessed a unique PubMLST id number (Table S1) [32].

Nucleotide sequence-based species identification

To identify Neisseria species based on their nucleotide sequences, this study used: (i) the rMLST scheme based on 53 ribosomal genes and (ii) the rplF allele number from the PubMLST platform.

Additional datasets

From de Block et al., WGS data from all commensal Neisseria (n=21) and N. gonorrhoeae (n=5) were included. From the study of Manoharan-Basil et al. all N. cinerea WGS data (n=42) and other commensal Neisseria WGS data (n=946) were included, as well as all N. meningitidis data (n=109). A N. gonorrhoeae subset was created from N. gonorrhoeae genome assemblies dating from 1990 and 2019 only as used in Manoharan-Basil et al. (i) based on the same MLST type (MLST profiles: 11422, 11706, 1583, 7822 and 10 314, n=36) from de Block et al. and (ii) based on the year 2019 (n=117) and excluding the year 1990. If more than one WGS shared the same MLST profile and the same year, only one WGS was selected. WGS data from historical strains (1983) from ITM (sequencing and assembly performed as described above and uploaded to PubMLST.org/neisseria) and two complete N. gonorrhoeae reference strains, FA1090 (NC_002946.2, PubMLST ID 2855) and MS11 (CP078118.1), were also included.

In total, the complete additional dataset consisted of WGS from 1280 isolates and included commensal Neisseria spp. [n=1011, including N. cinerea (n=42)], N. meningitidis (n=109) and N. gonorrhoeae (n=158) genomes together with N. gonorrhoeae reference genomes (n=2) (Table S2).

Core genome (cg) multi locus sequence typing (MLST)

Blast Score Ratio Based Allele Calling Algorithm (ChewBBACA) (v 2.8.5) was used to create two different Core Genome (cg) Multi Locus Sequence Typing (MLST) profiles from the study genomes (n=119) together with: (i) the N. gonorrhoeae reference genomes (n=2) and the N. gonorrhoeae genomes from the Block et al. (n=5) resulting in a panel of 126 genomes, and (ii) the complete additional dataset described above (n=1280) resulting in a panel of 1399 genomes [33]. First, the N. gonorrhoeae FA1090 reference genome was trained with prodigal [34]. A study-specific gene-by-gene schema was created by using a reference dataset comprised of 11 complete genomes from Manoharan-Basil et al. that included eight different Neisseria species (N. cinerea, N. elongata, N. meningitidis, N. polysaccharea, N. mucosa (including one genome which was previously identified as N. sicca), N. gonorrhoeae (FA1090 and MS11), N. subflava (including one genome which was previously identified as N. flavescens) and N. lactamica (Table S2, column E). This study-specific schema was used to call alleles on genomes of the two panels (panel n=126 and panel n=1399). From both allelic profiles, a set of loci that constitute the core genome was determined with threshold set on 0.95 and paralogs excluded.

In this way, two different gene-by-gene cgMLST profiles were created from both panels described above. Minimum spanning tree algorithm (MSTree V2) implemented in Grapetree was used to visualize the cgMLST allelic clusters, with collapsed branches set to 100 for Fig. 1a, b and c and 500 for Fig. 1d [35]. Labels in the figure were created using BioRender.

Hierarchical clustering of ribosomal genes

A project was created in PubMLST using all genomes in this study (n=119), reference strains FA1090 (PubMLST ID 2855) and all N. cinerea species (n=42) from the additional dataset as described above. From these genomes, rMLST genes (n=53) were extracted, concatenated and aligned by MAFFT (v 7.471) [36]. A maximum-likelihood (ML) phylogenetic tree was inferred from the alignment using IQ-TREE (v 2.2.5) with the MFP model, which automatically selects the best-fit substitution model using ModelFinder [37]. Branch support for the ML phylogeny was assessed with 1 000 standard non-parametric bootstrap analyses. The same approach was used to extract the rplF gene from N. cinerea genomes (n=41; one N. cinerea genome was excluded, which did not contain a full length rplF gene) and study genomes (n=119). Interactive tree of life (iTOL) was used to visualize both trees [38].

Pan and core genome visualization

The de novo assembled N. cinerea contigs from this study (n=5), and genomes from the additional dataset (n=42) were annotated with prokka 1.14.6 and the resulting gff3 annotation files were used as input for the pan genome pipeline roary (3.13.0) using default parameters to create a core-gene-alignment file and a gene presence and absence output file [39]. FastTree (v 2.1.10) was used to generate an approximately-maximum-likelihood phylogenetic tree from the alignment [40]. Phandango v 1.3.0 was used to jointly visualize the tree, gene presence-absence and metadata files [41].

Average Nucleotide Identity (ANI) calculation

The de novo assembled N. cinerea contigs from this study (n=5), and the additional dataset (n=42) were reordered using the complete genome sequence of N. cinerea (GenBank accession no: CP065726.1). Using default parameters, whole genome alignments were created using the Whole Genome Alignment plugin implemented in CLC Genomics Workbench (v 20). Average nucleotide identity (ANI) workflow was run with minimum similarity fraction and minimum length fraction set to 0.8. The csv output (Table S4) was used for further analysis in R (v 4.2.0).

Genome length, CDS counts, repeat sequences, virulence genes identification and recombination prediction

Genome length and CDS counts were inferred from prokka gff3 files. BLASTn v 2.11.0+ was used to search for DNA uptake sequence locations (AT)DUS (5'-ATGCCGTCTGAA-3') and Correia repeat enclosed elements CREE (5'-AGTGGATTAACAAAAACCAGTACGG CGTTGCCTCGCCTTAGCTCAAAGAGAACGATTCTCTAAGGTGCTGAAGCACTAAGTGAATCGGTTCCGTACTA TTTGTACTGTCTGCGGCTTCGTCGCCTTGTCCTGATTTTTGTTAATCCACTATAT-3') [42]. A Mann-Whitney U test was performed in R (v 4.2.0) for statistical analysis to evaluate differences between 'N. cinerea cluster one' and 'N. cinerea cluster two' of the continuous variables: (i) genome length, (ii) CDS, (iii) DUS and (iv) CREE. Abricate v1.01 was used to search for virulence genes from the genome assemblies (.fna files) using the VFDB database [43–45]. The resulting table shows the percentage coverage for genes which match genes from the Abricate database when the exact nucleotide matches is above 80%. Using blast, lbpA, lbpB, tbpA, tbpB and pilU genes were extracted, and an alignment from each gene was created with MAFFT and used as an input for IQ-TREE. Grapetree was used to visualise the tree. Based on the tree, sequences within the cluster of N. meningitidis and N. cinerea cluster two were used as an input for RDP4 v 4.101to predict recombination events [46].

Antimicrobial susceptibility determination, oxidase and Analytical Profile Index (API) tests of N. cinerea isolates

Minimum inhibitory concentrations (MICs) of N. cinerea isolates (n=5) from the study to azithromycin, ceftriaxone and ciprofloxacin were determined using E-test (BioMérieux, France), according to the manufacturer's instructions, on GC Chocolate agar plates (Becton Dickinson). In addition, all N. cinerea isolates from the study were tested for oxidase activity and inoculated on the API-NH v4.0 strip (BioMérieux).

Scanning electron microscopy (SEM)

Secondary electron (SE) scanning electron microscopy (SEM) images of N. cinerea clusters were acquired using a Thermo Fisher Scientific Quanta 250 FEG environmental SEM. The microscope was operated at 5 kV with a chamber pressure of 40 Pa. A 0.5 McFarland N. cinerea suspension were deposited and dried on a Si wafer at room temperature. Prior to the measurement, an 8 nm thick gold layer was deposited on the samples by a sputter coater (Leica Microsystems) to reduce charging effects.

Results

Identification of Neisseria species

Identification methods

MALDI-TOF MSAll 119 isolates were previously identified by MALDI-TOF MS (Table S3) [24]. Of these isolates, a high confidence score (score >2.0) was obtained for N. subflava (n=62), N. meningitidis (n=23), N. oralis (n=8), N. cinerea (n=3), N. elongata (n=3), N. mucosa (n=3), N. lactamica (n=2), and N. bacilliformis (n=1). For some isolates (n=14), MALDI-TOF MS resulted in a low confidence identification score (score 0.00–1.69) that included N. mucosa (n=10), N. meningitidis (n=2, isolates 19061666_1 and 19091461_1) and N. subflava (n=1, isolate 19040874_1, Table 1).

ID	MALDI-TOF MS	rMLST identification	rplF species annotation (allele nr)
19040874_1	*N. subflava*	*N. mucosa*	*N.* sp. *(201)*
19061666_1	*N. meningitidis*	*N. cinerea*	*N. cinerea (187)*
19091461_1	*N. meningitidis*	*N. cinerea*	*N. cinerea (187)*
Co000790_1	*N. meningitidis*	*N. polysaccharea*	*N. polysaccharea (44)*

Table 1.

Results of the identification of Neisseria species by MALDI-TOF MS, rMLST and rplF allele number of isolates which showed discrepancy among the different typing methods

Ribosomal multilocus sequence typing (rMLST)

After whole genome sequencing and de novo assembly, rMLST was used to identify all Neisseria spp. isolates (n=119). Four isolates showed discordant results compared to the MALDI-TOF MS results. Four isolates which were identified as N. meningitidis (n=3) and N. subflava (n=1) by MALDI-TOF MS, respectively were identified as N. polysaccharea (n=1), N. cinerea (n=2) and N. mucosa (n=1) by rMLST (Table 1 and S3).

Single gene species identification

When using the single marker rplF gene, it was possible to annotate all 119 isolates except two (Table S3). Of these 119 isolates, eighteen isolates were classified as 'Neisseria spp.' and twenty-three did not perfectly align with a rplF allele and showed a 'closest match' result. One isolate displayed a 'closest match' with a N. bergeri rplF allele but was identified as N. subflava according to MALDI-TOF MS and rMLST. All the other identifications concurred with the rMLST results.

Addressing the discrepancy among the different typing methods

To further investigate discrepancies in the various species identification methods, we conducted a detailed examination of the cgMLST profiles. The study-specific schema resulted in 934 cgMLST loci, and the MS tree was generated and categorized based on the different species identification

approaches, including MALDI-TOF MS (Fig. 1a), rMLST (Fig. 1) and rplF (Fig. 1c). Notably, isolate 19040874_1, which was initially classified as N. subflava by MALDI-TOF MS and N. mucosa by rMLST clustered within the N. mucosa clade (Fig. 1a and b). Isolate Co000790_1, identified as N. meningitidis by MALDI-TOF MS and as N. polysaccharea by rMLST and rplF approaches, is neighbouring with the N. polysaccharea reference (Fig. 1a, b and c). Additionally, isolates 19061666_1 and 19091461_1 appeared as a distinct N. cinerea cluster beside another N. cinerea cluster (Fig. 1b and c).

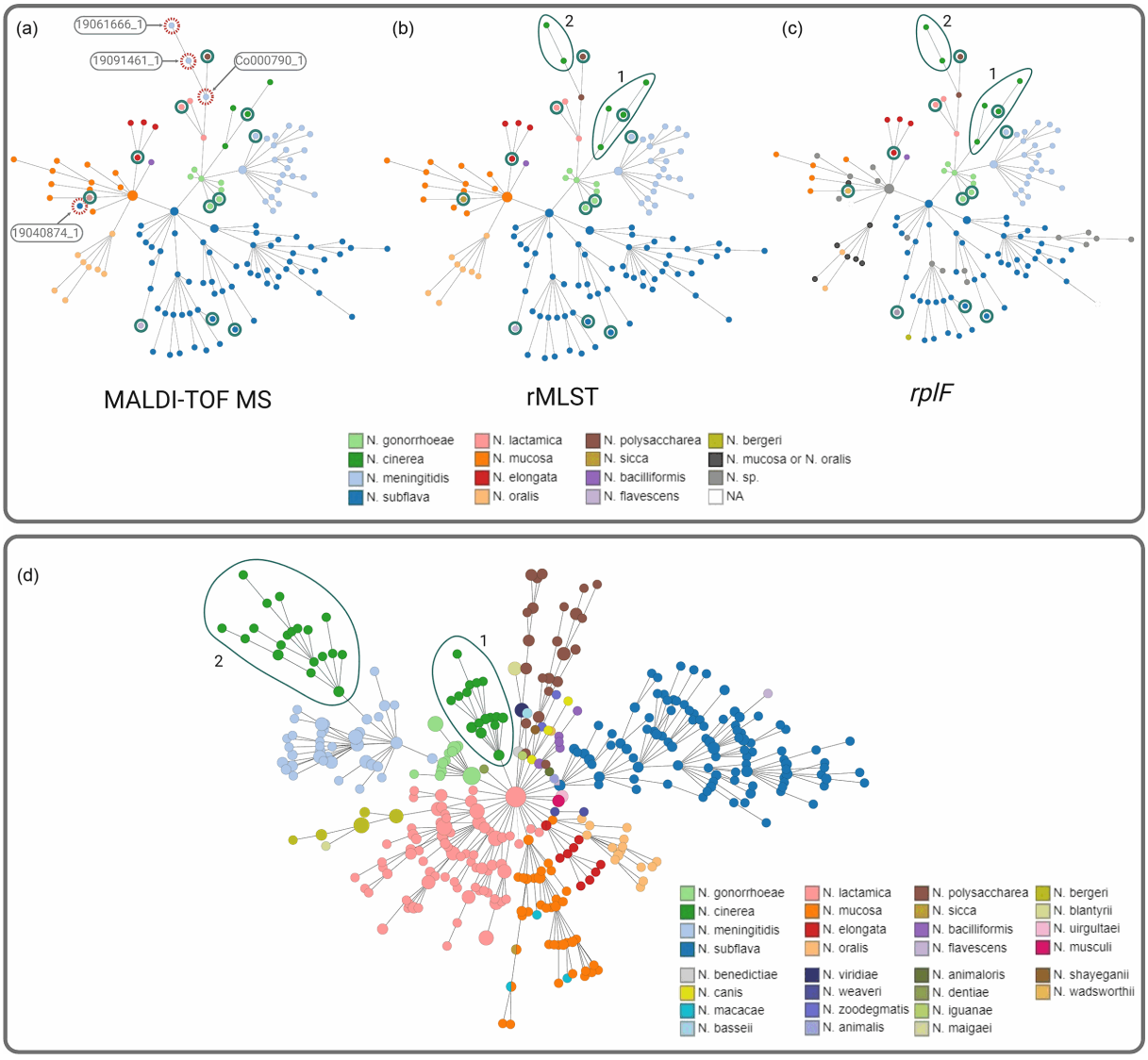

Fig. 1.

a, b and c: Identification of Neisseria species. Minimum spanning tree of cgMLST profiles (934 loci) generated with chewBACCA using study isolates (n=119), reference genomes (n=11, circled in green) and N. gonorrhoeae genomes (n=5, from de Block et al.). Isolates that were mis-identified with MALDI-TOF MS are labelled in panel A. Species are coloured by annotation (using previously used species name; N. flavescens and N. sicca) as identified with MALDI-TOF MS (a), rMLST typing (b) and rplF annotation (c). Isolates with different annotation by MALDI-TOF MS compared to rMLST are circled in red dashed lines. The two clusters of N. cinerea are numbered as one and two in the green shaded areas. d: Minimum spanning tree of cgMLST profiles generated with chewBACCA based on a 922 loci scheme. Presented are genomes from this study including publicly available Neisseria genomes

(n=1399). Different clusters of N. cinerea are indicated by green shaded area with cluster number (one or two).

Considering the congruence between the rMLST and rplF gene approaches for the isolates misidentified using MALDI-TOF MS and a more logical clustering based on the cgMLST tree, we employed genotypic species identification as species identifier for all the isolates (Table S1). This refinement resulted in a Neisseria genome dataset composed of the following species: N. meningitidis (n=23), N. subflava (n=61), N. mucosa (n=15), N. oralis (n=8), N. cinerea (n=5), N. elongata (n=3), N. lactamica (n=2), N. bacilliformis (n=1) and N. polysaccharea (n=1).

Taxonomic relationship of Neisseria species

The approach described above, revealed the presence of two distinct N. cinerea clusters as shown in Fig. 1b and c. To gain a more comprehensive understanding of these N. cinerea clusters, we included additional datasets (n=1280) to the study isolates (n=119). The inclusion of these isolates allowed us to obtain a more comprehensive overview of genomic variation between species. This resulted in 922 cgMLST loci that were generated from 1399 Neisseria spp. The cgMLST tree further confirmed the segregation of N. cinerea into two distinct clusters, referred to as 'N. cinerea cluster one' and 'N. cinerea cluster two' with a loci distance of 5328 (Fig. 1d). More specifically, 24 N. cinerea genomes grouped in cluster one and 23 N. cinerea genomes grouped in cluster two (Supplemental Data file – Table S5). Interestingly, the N. cinerea isolates from our study (n=5) were distributed in both clusters. Three N. cinerea isolates from the general population belonged to cluster one and two N. cinerea isolates from the MSM cohort belonged to cluster two.

Genotypic characterization of N. cinerea

Phylogenetic relationship of Neisseria species

A phylogenetic approach was used to further investigate the relationships among the two N. cinerea clusters. Two unrooted phylogenetic ML trees were created using (i) rMLST genes and (ii) rplF nucleotide sequences from N. cinerea genomes from the additional dataset (n=42) and the study isolates (n=119), including N. gonorrhoeae FA1090 reference (Fig. 2). The phylogenetic ML tree that was generated using the ribosomal sequences revealed two distinct clusters with high (100%) bootstrap branch support, within the N. cinerea clade (Fig. 2a). N. cinerea genomes were similarly divided over cluster one and cluster two as ascertained in the N. cinerea clusters from Fig. 1d.

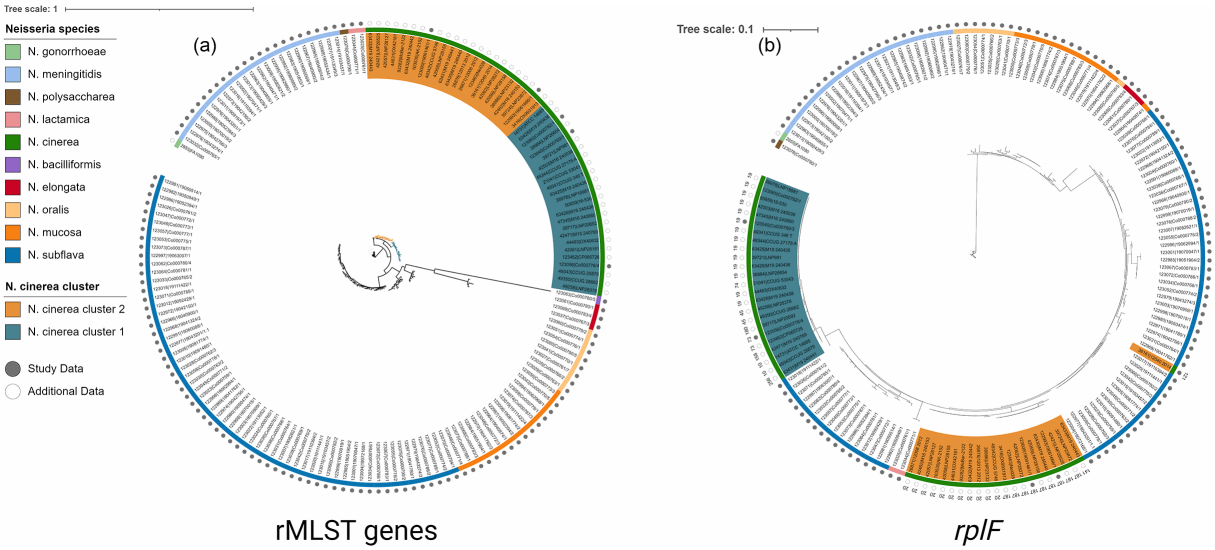

Fig. 2.

Unrooted maximum likelihood phylogeny tree based on alignment of 53 concatenated rMLST genes (a) and rplF gene (b). The coloured ring indicates the Neisseria species based on rMLST typing. The genomes of N. cinerea are labelled based on the cluster (green/teal: N. cinerea cluster one; and yellow: N. cinerea cluster two). Genome data from this study is indicated by a filled circle.

The rplF tree revealed the following structure in N. cinerea: rplF alleles of N. cinerea resulted in distinct clusters between rplF alleles from N. cinerea cluster one and N. cinerea cluster two, whereas one rplF allele of N. cinerea cluster two was separated from other rplF alleles from N. cinerea (Fig. 2b). In addition, rplF alleles were strictly divided between the clusters. Where cluster one included rplF allele numbers 10 (n=2), 19 (n=14), 45 (n=2), 73 (n=2), 74 (n=1), 158 (n=1), 180 (n=1), cluster two included numbers 20 (n=11), 121 (n=1), 141 (n=1), 187 (n=9), 256 (n=1, Fig. 2b and Supplemental Data file – Fig. S2). All of these rplF alleles resulted in genospecies N. cinerea except allele 141 and 256 of which no species annotation was provided (Table S3).

Pan genome comparison of N. cinerea

Core and accessory genes of N. cinerea genomes from this study (n=5) together with N. cinerea genomes (n=42) from the additional datasets were determined by Roary [39]. The presence and absence matrix of core and accessory genes showed the same separation of the N. cinerea genomes (Fig. 3). Furthermore, metadata showed that these clusters could not be grouped based on location or year. There were more invasive isolates from cluster two (n=5) compared to cluster one (n=1), although for most of the isolates this data was absent (Fig. 3).

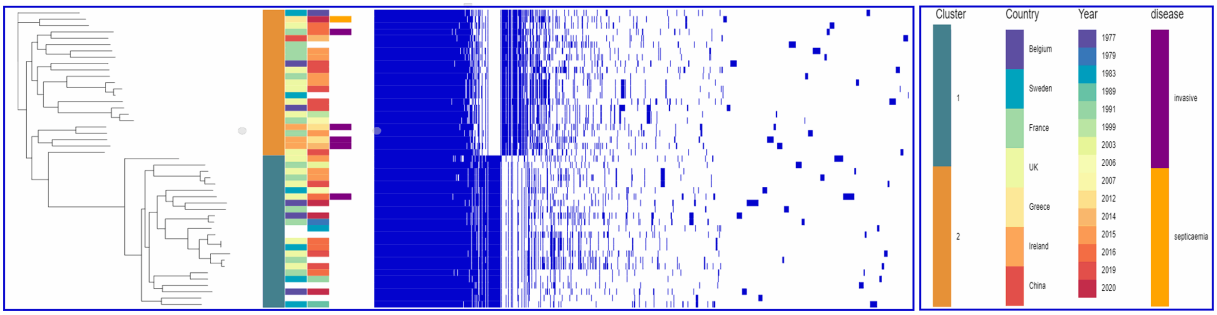

Fig. 3.

Visualization of the pan genome using phandango of N. cinerea genomes (n=47). Phylogenetic tree is based on the core genome sequences. Isolates are labelled with cluster, country, year and disease with corresponding gene presence absence matrix. Blank indicates the absence of the metadata or gene. The five isolates from Belgium are all from this study.

Average nucleotide identity of N. cinerea clusters

When comparing different clusters (inter cluster), the ANI values ranged between 93.1 and 93.8% (median: 93.31; IQR 93.25–93.36) (Fig. 4). However, when comparing sequences within the same cluster (intra cluster), the ANI values were notably higher, ranging from 96.3–99.99% (median: 97.13; IQR 96.88–97.12) for cluster one and from 96.0–99.6% for cluster two (median: 96.37; IQR 96.18–96.38). In other words, the comparison between different clusters of N. cinerea showed average nucleotide identity (ANI) percentages sequence identities below the 95% species boundaries [47]. Additionally, a positive correlation was observed between the alignment percentage (AP) and ANI values, where the more distantly related species exhibited a lower proportion of sequence aligned, while the closely related species showed a higher sequence alignment percentage (Fig. 4). Using the arbitrary cutoff value of 95% for species identification [47], the two clusters of N. cinerea could be considered as two distinct species.

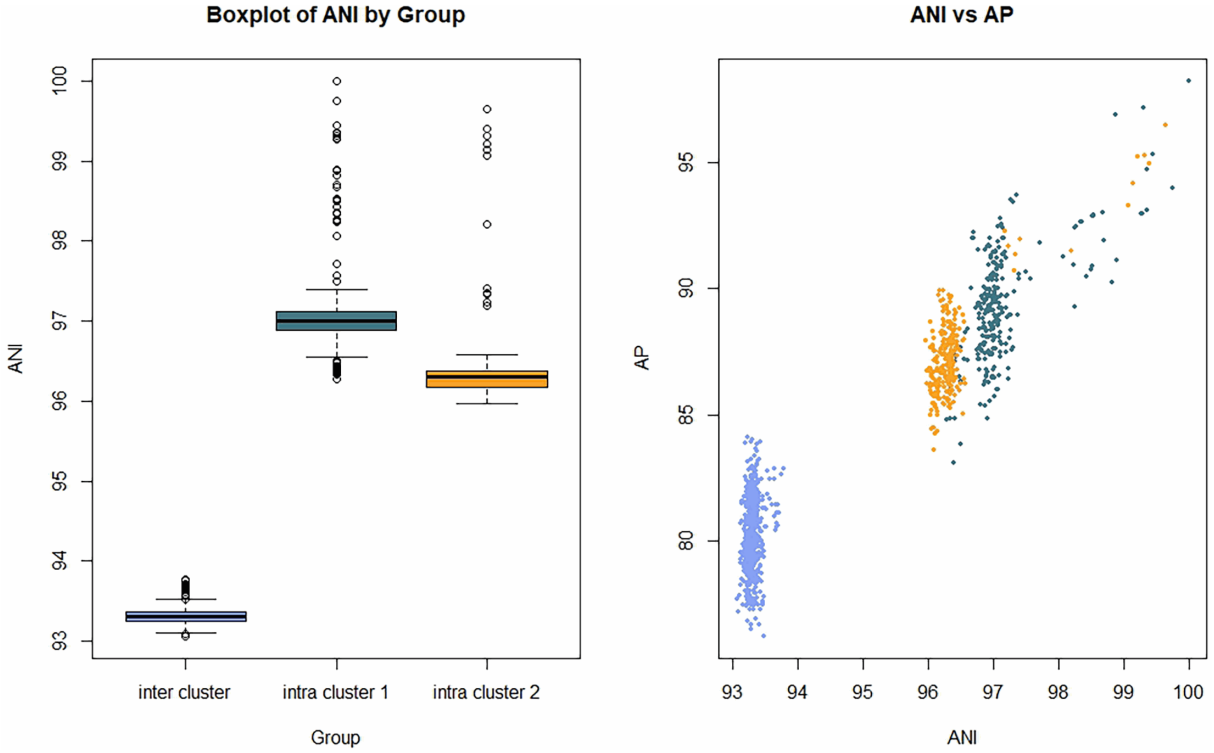

Boxplot of average nucleotide identity (ANI) results between and within each N. cinerea clusters and correlation plot of ANI vs alignment percentage (AP).

Genomic characteristics of N. cinerea 'cluster one' and 'cluster two'

CDS and genome length

The genomes from N. cinerea cluster one and N. cinerea cluster two had a median length of 1.89 Mb (IQR 1.87–1.94) and 2.02 Mb (IQR 1.99–2.06; p-value 3.68e-06), respectively. The number of CDS was higher in N. cinerea cluster two with a median of 1872 (IQR 1827–1910.5) compared to the CDS median of 1802.5 (1749.25-1849.75; p-value 0.007026) for N. cinerea cluster one.

Signatures of repeat sequences in N. cinerea

The extended 12 bp DUS (eDUS; 5'-ATGCCGTCTGAA-3') is the most abundant DUS dialect found in both N. cinerea clusters, which is also the same dialect as found in N. meningitidis [48]. N. cinerea cluster two, however, had more copies of AT-DUS than cluster one (median copy number of 2238 (IQR 2207.5–2261.5) and 2006.5 (IQR 1958.25–2021.5; p-value 4.536e-09) respectively. A higher copy number of the CREE, was detected in N. cinerea cluster two than one (median of 116 (IQR 108–122) and 12; IQR 10–14; p-value=4.314e-09 respectively; Table 2).

	N. cinerea cluster one	*N. cinerea* cluster two
Genome length (Mb)	1.89 (IQR 1.87–1.94)	2.02 (IQR 1.99–2.06)
CDS (nr)	1802.5 (1749.25–1849.75)	1872 (IQR 1827–1910.5)
ATDUS (nr)	2006.5 (IQR 1958, 25–2021.5)	2238 (IQR 2207.5–2261.5)
CREE (nr)	12 (IQR 10–14)	116 (IQR 108–122)

Table 2.

Genomic characteristics of N. cinerea cluster one and two: Genome length, CDS, AT-DUS and CEI

Virulence genes in N. cinerea cluster one and cluster two

By using the virulence factor database, containing virulence factors of pathogenic bacteria, up to 33 different virulence genes, genetical similar to N. meningitidis (based on 80% or more exact nucleotide matches), were detected in N. cinerea genomes (Table S6). Some of these virulence genes were only frequently observed in genomes from cluster two (hmbR, n=12; lbpB, n=21; nspA, n=7; pilU, n=23; tbpA, n=23; tbpB, n=15) and one only in cluster one (pilM, n=22).

To verify the presence of more distantly related alleles of these 33 virulence genes, a presence/absence table was created in pubMLST (Table S7). This analysis showed discrepancy between the clusters by the presence of hmbR or hpuAB. Genomes from cluster one contained only the hpuAB gene, while most genomes from cluster two only contained hmbR (20 out of 23 genomes). For all other virulence genes, different alleles were present in both clusters.

Because of their importance in virulence, more detailed phylogenetic analyses were performed on five virulence genes which were present in both clusters but found to be more genetically identical to N. meningitidis in cluster two. These concerned the genes pilU, transferrin binding proteins (tbpA and tbpB) and lactoferrin binding proteins (lbpA and lbpB). Phylogenetic relationship analysis of each of these genes separately confirmed that each of these genes from cluster two were more closely related to N. meningitidis than to cluster one (Supplemental Data file – Fig. S3). In most cases, genes from cluster two and genes from N. meningitidis were clustered and separated by long branches from cluster one genes. Recombination analysis from each of these five genes revealed the occurrence of several recombination events between N. meningitidis and cluster two in tbpA, tbpB, lbpA and lbpB (Supplemental Data file – Figs S4–S7, Table S9). No recombinations were predicted for pilU.

Phenotypic characterization of N. cinerea isolates

Minimum inhibitory concentrations (MIC) and biochemical tests of N. cinerea isolates

The azithromycin, ceftriaxone and ciprofloxacin MICs were determined for the N. cinerea isolates from this study (n=5). There was no significant difference in the MIC values for any of these antibiotics between the clusters.

Biochemical characteristics of the N. cinerea isolates from this study (N. cinerea cluster one, n=3; N. cinerea cluster two, n=2) were determined by two biochemical tests: API NH and oxidase test. There were no differences between the clusters, and all biochemical profiles corresponded with the N. cinerea profile (API NH profile 0001, oxidase-negative; Table 3).

ID	cl	MIC AZM	MIC CRO	MIC CIF	PEN	GLU	FRU	MAL	SAC	ODC	URE	LIP	PAL	βGAL	ProA	GGT	IND	OT
19061666_1	2	3	1	0,064	–	–	–	–	–	–	–	–	–	–	+	–	–	–
19091461_1	2	6	0,008	0,008	–	–	–	–	–	–	–	–	–	–	+	–	–	–
Co000766_4	1	1	0,008	0,006	–	–	–	–	–	–	–	–	–	–	+	–	–	–
Co000769_3	1	24	0,008	0,032	–	–	–	–	–	–	–	–	–	–	+	–	–	–
Co000782_1	1	2	0,008	0,012	–	–	–	–	–	–	–	–	–	–	+	–	–	–

Table 3.

Characteristics of N. cinerea isolates from cluster one and cluster two (cl) in this study. Minimum inhibitory concentrations (MIC) of azithromycin (AZM), ceftriaxone (CRO) and ciprofloxacin (CIF) were determined. API NH V4.0 (PEN: penicillinase; GLU: glucose; FRU: fructose; MAL: maltose; SAC: saccharose; URE: urea; LIP: lipase; PAL: alkaline phosphatase; βGAL: β-galactosidase; ProA: proline arylamidase; GGT: gamma-glutamyl transferase; IND: indole) and oxidase test (OT) were used to determine the biochemical characteristics

Scanning electron microscopy of N. cinerea isolates

High resolution imaging with scanning electron microscopy (SEM) showed the classic diplococcal arrangement in all N. cinerea isolates assessed (n=4). No difference in the size was noted between the isolates from cluster one (n=2) and cluster two (n=2, Fig. 5). Some of the cluster one isolates may appear to have more membrane particles compared to cluster two. All images are provided in Supplemental Data file Fig. S8.

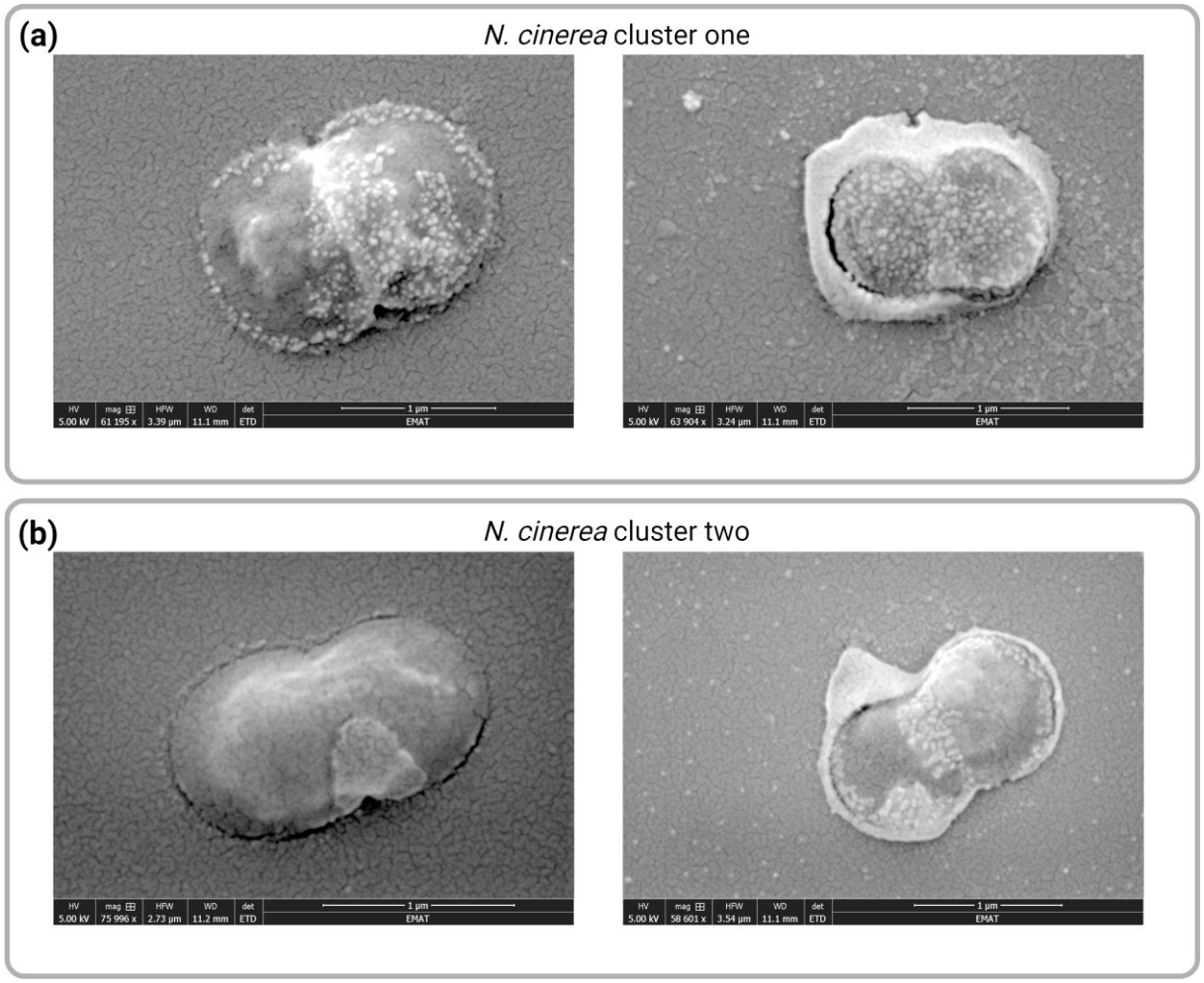

Fig. 5.

Scanning electron microscopy (SEM). Images of N. cinerea cluster one isolates Co000782_1 and Co000769_3 (panel a) and N. cinerea cluster two isolates 19091461_1 and 19061666_1 (panel b). The white line below in every image represents a scale of 1 µM.

Discussion

This genomic surveillance study of oropharyngeal Neisseria species in Belgium has two main findings. First, the use of MALDI-TOF MS for the identification of Neisseria species results in the misidentification of several Neisseria species, including N. cinerea, N. mucosa and N. polysaccharea as N. meningitidis and N. subflava. Second, N. cinerea is comprised of two clusters based on WGS, cgMLST and phylogenetic analysis of individual genes. Further phylogenetic analysis, including additional public N. cinerea genomic data, confirmed that N. cinerea is polyphyletic and is comprised two distinct lineages, designated cluster one and two.

The most significant misidentification by MALDI-TOF MS was of two N. cinerea cluster two isolates as N. meningitidis. In the same cluster, four N. cinerea isolates (pubMLST ID: 42057, 42 058, 42 059 and 42 421) were also reported as being misidenitified as N. meningitidis by MALDI-TOF MS [15]. The two N. cinerea cluster two isolates from our study, were obtained from the MSM cohort. N. meningitidis was more frequently detected in the MSM cohort (22/64 individuals) than in the general population (1/32 individuals). This high prevalence of N. meningitidis in MSM is similar to that found in other

studies [49]. If N. meningitidis and N. cinerea cohabit the same niche in the same cohort, then it would be possible for N. meningitidis and N. cinerea to exchange parts of their genome. Although speculative and based on small numbers, this offers one explanation for why the cluster two N. cinerea detected in MSM could be misidentified as N. meningitidis.

Misidentification of non-Neisseria meningitidis species can result in inappropriate diagnoses and therapies and has consequences for public health surveillance and lab management [8, 50]. Commensal Neisseria can occasionally cause infections, mostly within immunocompromised or immunosuppressed patients, but are less susceptible to several antibiotics compared to pathogenic Neisseria [8, 51]. Moreover, they may be the source of resistance to multiple classes of antibiotics for pathogenic Neisseria [9–12]. Misidentification of commensal Neisseria once infectious, can have consequences for selecting an effective antibiotic and dose, hence can lead to treatment failure.

Studies have indicated that improving MALDI-TOF MS mass spectral quality (MSQ) and improving incomplete databases are essential for increasing the resolution of bacterial identification [52]. The false-positive diagnosis of N. meningitidis by MALDI-TOF MS of N. cinerea and N. polysaccharea isolates in our study, appears to be a recurrent issue, as previously described [15–17, 19]. Other reported misidentifications among Neisseria spp. by MALDI-TOF MS included N. bergeri and N. subflava [15, 18]. The accuracy of MALDI-TOF MS can be affected by factors such as inherent similarities between organisms. Particularly in the case of the Neisseria genus with high inter-species recombination. Additionally, the limited number of commensal Neisseria spectra in the database [53, 54]. Our findings indicate that MALDI-TOF MS algorithms require improvements for Neisseria species identification using large, well-characterized and varied representative panels of commensal and pathogenic Neisseria species isolates.

The polyphyletic population structure of N. cinerea was substantiated by both phylogenetic and ANI analyses. ANI analysis revealed a bimodal ANI distribution (Fig. 4). The different N. cinerea clusters showed ANI percentage sequence identities below the 95% species boundaries (Fig. 4), suggestive of a new species [47]. However, we were unable to identify any phenotypic differences between the two clusters. In addition, the presence of extensive inter-species genomic recombination within the Neisseria genus, can lead to taxonomic confusions [55–60]. Comparative analysis of genome characteristics between the N. cinerea clusters revealed that cluster two had a bigger genome size, a higher number of coding sequences, and contained more repeat sequences. We also found several genes in cluster two genetically similar to the virulence genes from N. meningitidis. A number of recombination events between N. meningitidis and cluster two were found in these virulence genes. Since some of these virulence proteins, such as TbpA and NspA, are surface exposed and may be expressed in outer membrane vesicles they are important vaccine targets [61, 62]. Frequent recombination between N. meningitidis and cluster two in the genes coding these proteins has two important consequences for meningococcal vaccines. First, the vaccine may reduce the prevalence of cluster two and place a selective pressure on the emergence of escape mutants. Secondly, future recombination could transfer the DNA coding vaccine escape from cluster two to N. meningitidis [63, 64].

We detected different haem transport systems in each cluster. Cluster two genomes contained hmbR only, which extracts haem from haemoglobin, while the hpuAB system, which processes haem from haemoglobin, haptoglobin, and hemoglobin-haptoglobin complexes, was present in cluster one genomes only [65]. Distinct distributions of hmbR/hpuAB genes has also been described in N. meningitidis, where isolates possessing hmbR are predominantly associated with invasive disease with meningococci obtained from carriage generally lacking the hmbR gene but possessing hpuAB [66]. More recently, meningococci associated with invasive disease and lacking hmbR have been described

in France indicating that hmbR distribution in the Neisseria genus is dynamic [67]. The dichotomy of hmbR/hpuAB between both N. cinerea clusters and the description of capsule biosynthesis genes in some commensal Neisseria species warrants enhanced genomic surveillance [68]. Thus, not only is it important to detect AMR sequences in commensals which could emerge in pathogenic Neisseria via HGT, genomic surveillance of commensals will also be important in enhancing our understanding of the impact of vaccination in the Neisseria genus.

We acknowledge that our study is not without limitations. The samples from both Belgian cohorts were not nationally representative samples but rather from individuals attending a single medical centre in Belgium. Although we included all the N. cinerea isolates with WGS available world-wide, we still had a small sample size (n=47). We were only able to evaluate five of these phenotypically, which were isolated in our centre. There were also a number of apparent gaps in the coverage of the global isolates. For example, there were no samples from sub-Saharan Africa. Furthermore, it would be particularly useful to conduct phenotypic and genotypic surveillance of commensal Neisseria in populations that are most prone to the emergence of AMR in N. gonorrhoeae such as MSM in PrEP cohorts and sex workers [69–71]. Surveillance studies of commensal Neisseria spp. in Japan and elsewhere have, for example, clearly revealed that commensal Neisseria were the source of mosaic penA genes that conferred resistance to extended spectrum cephalosporins and macrolides [72, 73]. In addition to this, generating complete genomes based on long reads, might provide additional insights into intra- and inter-species recombination, repeat sequences and genome arrangement. Another limitation is that we did not quantitatively assess if there were significant differences in membrane particles observed in the SEM images between N. cinerea cluster one and cluster two, as this was beyond the scope of the current study. In summary, future surveillance studies could include: (i) globally collected isolates, (ii) populations with high risk of antibiotic resistant strains and (iii) long-read sequencing of isolates. Finally, there is a need for prospective studies to estimate the prevalence of missed diagnoses via MALDI-TOF MS.

Conclusions

The integration of multiple methods revealed two distinct N. cinerea clusters that challenge taxonomic boundaries and provided valuable insights into Neisseria commensal species genetic diversity and virulence potential. These findings have implications for clinical diagnostics and public health, emphasizing the importance of continued research in this field.

Funding information

This research was supported by SOFI 2021 grant—'PReventing the Emergence of untreatable STIs via radical Prevention' (PRESTIP).

Acknowledgements

We would like to thank all the study participants for their help in this study. This research was supported by SOFI 2021 grant—'PReventing the Emergence of untreatable STIs via radical Prevention' (PRESTIP).

Author contributions

T.d.B., C.K., S.S.M.B. and O.H. conceptualised the study; S.A., C.K., C.V.D. and J.L. collected the samples; S.A., Z.G., J.L., and I.D.B. processed the samples; S.A., Z.G. and N.C. generated the laboratory results; T.d.B., O.H. and S.S.M.B. performed bioinformatic analyses; T.d.B., C.K., S.S.M.B., O.H. and K.V. interpreted the data; T.d.B. drafted the manuscript and created the figures; T.d.B., K.V., C.K., S.S.M.B. and O.H. edited, wrote and reviewed manuscript; all authors revised the manuscript and approved the final version.

Conflicts of interest

There are no conflicts of interest to declare.

Reference

de Block T, Laumen JGE, Van Dijck C, Abdellati S, De Baetselier I et al. Wgs of commensal Neisseria reveals acquisition of a new ribosomal protection protein (Msrd) as a possible explanation for high level azithromycin resistance in Belgium. Pathogens 2021; 10:384 [View Article] [PubMed] [Google Scholar]

Manoharan-Basil SS, González N, Laumen JGE, Kenyon C. Horizontal gene transfer of fluoroquinolone resistance-conferring genes from commensal Neisseria to Neisseria gonorrhoeae: a global phylogenetic analysis of 20,047 isolates. Front Microbiol 2022; 13:793612 [View Article] [PubMed] [Google Scholar]

Deasy AM, Guccione E, Dale AP, Andrews N, Evans CM et al. Nasal inoculation of the commensal Neisseria lactamica inhibits carriage of neisseria meningitidis by young adults: a controlled human infection study. Clin Infect Dis 2015; 60:1512–1520 [View Article] [PubMed] [Google Scholar]

Lu M, Xuan S, Wang Z. Oral microbiota: a new view of body health. Food Sci Hum Wellness 2019; 8:8–15 [View Article] [Google Scholar]

Custodio R, Johnson E, Liu G, Tang CM, Exley RM. Commensal Neisseria cinerea impairs Neisseria meningitidis microcolony development and reduces pathogen colonisation of epithelial cells. PLoS Pathog 2020; 16:1–21 [View Article] [PubMed] [Google Scholar]

Rosier BT, Moya-Gonzalvez EM, Corell-Escuin P, Mira A. Isolation and characterization of nitrate-reducing bacteria as potential probiotics for oral and systemic health. Front Microbiol 2020; 11:1–19 [View Article] [PubMed] [Google Scholar]

Dorey RB, Theodosiou AA, Read RC, Jones CE. The nonpathogenic commensal Neisseria: friends and foes in infectious disease. Curr Opin Infect Dis 2019; 32:490–496 [View Article] [PubMed] [Google Scholar]

Walsh L, Clark SA, Derrick JP, Borrow R. Beyond the usual suspects: reviewing infections caused by typically-commensal Neisseria species. J Infect 2023; 87:1–11 [View Article] [PubMed] [Google Scholar]

Kenyon C, Laumen J, Manoharan-Basil S. Choosing new therapies for Gonorrhoea: we need to consider the impact on the pan-Neisseria genome. a viewpoint. Antibiotics 2021; 10:515 [View Article] [PubMed] [Google Scholar]

Goytia M, Wadsworth CB. Canary in the coal mine: how resistance surveillance in commensals could help curb the spread of AMR in pathogenic Neisseria. mBio 2022; 13:e0199122 [View Article] [PubMed] [Google Scholar]

Kanesaka I, Ohno A, Morita M, Katsuse AK, Morihana T et al. Epigenetic effects of ceftriaxone-resistant Neisseria gonorrhoeae FC428 mosaic-like sequences found in PenA sequences unique to Neisseria subflavaand related species. J Antimicrob Chemother 2023; 78:1–8 [View Article] [PubMed] [Google Scholar]

Unitt A, Maiden M, Harrison O. Characterizing the diversity and commensal origins of penA mosaicism in the genus Neisseria. Microbial Genomics 2024; 10:1–12 [View Article] [Google Scholar]

Jolley KA, Bliss CM, Bennett JS, Bratcher HB, Brehony C et al. Ribosomal multilocus sequence typing: universal characterization of bacteria from domain to strain. Microbiology 2012; 158:1005–1015 [View Article] [PubMed] [Google Scholar]

Bennett JS, Watkins ER, Jolley KA, Harrison OB, Maiden MCJ. Identifying Neisseria species by use of the 50S ribosomal protein L6 (rplF) gene. J Clin Microbiol 2014; 52:1375–1381 [View Article] [PubMed] [Google Scholar]

Hong E, Bakhalek Y, Taha MK. Identification of Neisseria meningitidis by MALDI-TOF MS may not be reliable. Clin Microbiol Infect 2019; 25:717–722 [View Article] [PubMed] [Google Scholar]

Kawahara-Matsumizu M, Yamagishi Y, Mikamo H. Misidentification of Neisseria cinerea as Neisseria meningitidis by Matrix-Assisted Laser Desorption/Ionization Time of Flight Mass Spectrometry (MALDI-TOF MS). Jpn J Infect Dis 2018; 71:85–87 [View Article] [PubMed] [Google Scholar]

Cunningham SA, Mainella JM, Patel R. Misidentification of Neisseria polysaccharea as Neisseria meningitidis with the use of matrix-assisted laser desorption ionization-time of flight mass spectrometry. J Clin Microbiol 2014; 52:2270–2271 [View Article] [PubMed] [Google Scholar]

Unalan-Altintop T, Karagoz A, Hazirolan G. A diagnostic challenge in clinical laboratory: misidentification of Neisseria subflava as Neisseria meningitidis by MALDI-TOF MS. Acta Microbiol Immunol Hung 2020; 67:258–260 [View Article] [PubMed] [Google Scholar]

von Kietzell M, Richter H, Bruderer T, Goldenberger D, Emonet S et al. Meningitis and bacteremia due to neisseria cinerea following a percutaneous rhizotomy of the trigeminal ganglion. J Clin Microbiol 2016; 54:233–235 [View Article] [Google Scholar]

Bennett JS, Jolley KA, Earle SG, Corton C, Bentley SD et al. A genomic approach to bacterial taxonomy: an examination and proposed reclassification of species within the genus Neisseria. . Microbiology 2012; 158:1570–1580 [View Article] [Google Scholar]

Bennett JS, Jolley KA, Maiden MCJ. Genome sequence analyses show that Neisseria oralis is the same species as “Neisseria mucosa var. Heidelbergensis.”. Int J Syst Evol Microbiol 2013; 63:3920–3926 [View Article] [PubMed] [Google Scholar]

Diallo K, MacLennan J, Harrison OB, Msefula C, Sow SO et al. Genomic characterization of novel Neisseria species. Sci Rep 2019; 9:13742 [View Article] [PubMed] [Google Scholar]

Mustapha MM, Lemos APS, Griffith MP, Evans DR, Marx R et al. Two cases of newly characterized Neisseria species, Brazil. Emerg Infect Dis 2020; 26:366–369 [View Article] [PubMed] [Google Scholar]

Laumen JGE, Van Dijck C, Abdellati S, De Baetselier I, Serrano G et al. Antimicrobial susceptibility of commensal Neisseria in a general population and men who have sex with men in Belgium. Sci Rep 2022; 12:1–10 [View Article] [PubMed] [Google Scholar]

Van Dijck C, Tsoumanis A, Rotsaert A, Vuylsteke B, Van den Bossche D et al. Antibacterial mouthwash to prevent sexually transmitted infections in men who have sex with men taking HIV pre-exposure prophylaxis (PReGo): a randomised, placebo-controlled, crossover trial. Lancet Infect Dis 2021; 21:657–667 [View Article] [PubMed] [Google Scholar]

Andrews S. A quality control tool for high throughput sequence data. n.d https://www.bioinformatics.babraham.ac.uk/projects/fastqc/

Bolger AM, Lohse M, Usadel B. Trimmomatic: a flexible trimmer for Illumina sequence data. Bioinformatics 2014; 30:2114–2120 [View Article] [PubMed] [Google Scholar]

Seemann T. shovill. n.d https://github.com/tseemann/shovill

Prjibelski A, Antipov D, Meleshko D, Lapidus A. Using spades de novo assembler. Curr Protoc Bioinforma 2020; 70: [View Article] [Google Scholar]

Gurevich A, Saveliev V, Vyahhi N, Tesler G. QUAST: quality assessment tool for genome assemblies. Bioinformatics 2013; 29:1072–1075 [View Article] [PubMed] [Google Scholar]

Seemann T. Prokka: rapid prokaryotic genome annotation. Bioinformatics 2014; 30:2068–2069 [View Article] [PubMed] [Google Scholar]

Jolley KA, Bray JE, Maiden MCJ. Open peer review open-access bacterial population genomics: BIGSdb software, the PubMLST.org website and their applications [version 1; peer review: 2 approved]. Wellcome Open Res 2018; 3:124 [View Article] [PubMed] [Google Scholar]

Silva M, Machado MP, Silva DN, Rossi M, Moran-Gilad J et al. chewBBACA: a complete suite for gene-by-gene schema creation and strain identification. Microb Genom 2018; 4:e000166 [View Article] [PubMed] [Google Scholar]

Hyatt D, Chen G-L, Locascio PF, Land ML, Larimer FW et al. Prodigal: prokaryotic gene recognition and translation initiation site identification. Nat Commun 2010; 6:1–8 [View Article] [PubMed] [Google Scholar]

Zhou Z, Alikhan N-F, Sergeant MJ, Luhmann N, Vaz C et al. GrapeTree: visualization of core genomic relationships among 100,000 bacterial pathogens. Genome Res 2018; 28:1395–1404 [View Article] [PubMed] [Google Scholar]

Katoh K, Standley DM. MAFFT multiple sequence alignment software version 7: improvements in performance and usability. Mol Biol Evol 2013; 30:772–780 [View Article] [PubMed] [Google Scholar]

Nguyen L, Schmidt HA, von Haeseler A, Minh BQ. IQ-TREE: a fast and effective stochastic algorithm for estimating maximum-likelihood phylogenies. Mol Biol Evol 2014; 32:268–274 [View Article] [Google Scholar]

Letunic I, Bork P. Interactive Tree Of Life (iTOL) v5: an online tool for phylogenetic tree display and annotation. Nucleic Acids Res 2021; 49:W293–W296 [View Article] [PubMed] [Google Scholar]

Page AJ, Cummins CA, Hunt M, Wong VK, Reuter S et al. Roary: rapid large-scale prokaryote pan genome analysis. Bioinformatics 2015; 31:3691–3693 [View Article] [PubMed] [Google Scholar]

Price MN, Dehal PS, Arkin AP. FastTree: computing large minimum evolution trees with profiles instead of a distance matrix. Mol Biol Evol 2009; 26:1641–1650 [View Article] [PubMed] [Google Scholar]

Hadfield J, Croucher NJ, Goater RJ, Abudahab K, Aanensen DM et al. Phandango: an interactive viewer for bacterial population genomics. Bioinformatics 2018; 34:292–293 [View Article] [PubMed] [Google Scholar]

Camacho C, Coulouris G, Avagyan V, Ma N, Papadopoulos J et al. BLAST+: architecture and applications. BMC Bioinformatics 2009; 10:1–9 [View Article] [PubMed] [Google Scholar]

Seemann T. Abricate. n.d https://github.com/tseemann/abricate

Krüger N-J, Stingl K. Two steps away from novelty--principles of bacterial DNA uptake. Mol Microbiol 2011; 80:860–867 [View Article] [PubMed] [Google Scholar]

Chen L, Zheng D, Liu B, Yang J, Jin Q. VFDB 2016: hierarchical and refined dataset for big data analysis—10 years on. Nucleic Acids Res 2016; 44:D694–D697 [View Article] [Google Scholar]

Martin DP, Murrell B, Golden M, Khoosal A, Muhire B. RDP4: detection and analysis of recombination patterns in virus genomes. Virus Evol 2015; 1:1–5 [View Article] [PubMed] [Google Scholar]

Jain C, Rodriguez-R LM, Phillippy AM, Konstantinidis KT, Aluru S. High throughput ANI analysis of 90K prokaryotic genomes reveals clear species boundaries. Nat Commun 2018; 9:1–8 [View Article] [PubMed] [Google Scholar]

Frye SA, Nilsen M, Tønjum T, Ambur OH. Dialects of the DNA Uptake Sequence in Neisseriaceae. PLoS Genet 2013; 9:e1003458 [View Article] [PubMed] [Google Scholar]

Ngai S, Weiss D, Bell JA, Majrud D, Zayas G et al. Carriage of Neisseria meningitidis in men who have sex with men presenting to public sexual health clinics, New York City. Sex Transm Dis 2020; 47:541–548 [View Article] [PubMed] [Google Scholar]

Deak E, Green N, Humphries RM. Microbiology test reliability in differentiation of Neisseria meningitidis and Neisseria polysaccharea. . J Clin Microbiol 2014; 52:3496 [View Article] [PubMed] [Google Scholar]

Goytia M, Thompson ST, Jordan SVL, King KA. Antimicrobial resistance profiles of human commensal Neisseria species. Antibiotics 2021; 10:538 [View Article] [PubMed] [Google Scholar]

Cuénod A, Aerni M, Bagutti C, Bayraktar B, Boz ES et al. Quality of MALDI-TOF mass spectra in routine diagnostics: results from an international external quality assessment including 36 laboratories from 12 countries using 47 challenging bacterial strains. Clin Microbiol Infect 2023; 29:190–199 [View Article] [PubMed] [Google Scholar]

Liébana-Martos C. Interpretation of results, advantages disadvantages, and limitations of MALDI-TOF. Use Mass Spectrom Technol Clin Microbiol 201875–86 [View Article] [Google Scholar]

Rychert J. Benefits and limitations of MALDI-TOF mass spectrometry for the identification of microorganisms. J Infect 2019; 2:1–5 [View Article] [Google Scholar]

Zong Z. Genome-based taxonomy for bacteria: a recent advance. Trends Microbiol 2020; 28:871–874 [View Article] [PubMed] [Google Scholar]

Murray CS, Gao Y, Wu M. Re-evaluating the evidence for a universal genetic boundary among microbial species. Nat Commun 2021; 12:1–5 [View Article] [PubMed] [Google Scholar]

Rodriguez-R LM, Jain C, Conrad RE, Aluru S, Konstantinidis KT. Reply to: “re-evaluating the evidence for a universal genetic boundary among microbial species.”. Nat Commun 2021; 12:4060 [View Article] [PubMed] [Google Scholar]

Hanage WP, Fraser C, Spratt BG. Fuzzy species among recombinogenic bacteria. BMC Biol 2005; 3:1–7 [View Article] [PubMed] [Google Scholar]

Corander J, Connor TR, O’Dwyer CA, Kroll JS, Hanage WP. Population structure in the Neisseria, and the biological significance of fuzzy species. J R Soc Interface 2012; 9:1208–1215 [View Article] [PubMed] [Google Scholar]

Hanage WP. Fuzzy species revisited. BMC Biol 2013; 11:10–12 [View Article] [PubMed] [Google Scholar]

Moe GR, Zuno-Mitchell P, Lee SS, Lucas AH, Granoff DM. Functional activity of anti-neisserial surface protein A monoclonal antibodies against strains of Neisseria meningitidis serogroup B. Infect Immun 2001; 69:3762–3771 [View Article] [PubMed] [Google Scholar]

Fegan JE, Calmettes C, Islam EA, Ahn SK, Chaudhuri S et al. Utility of hybrid transferrin binding protein antigens for protection against pathogenic Neisseria species. Front Immunol 2019; 10:1–4 [View Article] [PubMed] [Google Scholar]

Jolley KA, Wilson DJ, Kriz P, McVean G, Maiden MCJ. The influence of mutation, recombination, population history, and selection on patterns of genetic diversity in Neisseria meningitidis. Mol Biol Evol 2005; 22:562–569 [View Article] [PubMed] [Google Scholar]

Joseph B, Schwarz RF, Linke B, Blom J, Becker A et al. Virulence evolution of the human pathogen Neisseria meningitidis by recombination in the core and accessory genome. PLoS One 2011; 6:e18441 [View Article] [PubMed] [Google Scholar]

Perkins-Balding D, Ratliff-Griffin M, Stojiljkovic I. Iron transport systems in Neisseria meningitidis. Microbiol Mol Biol Rev 2004; 68:154–171 [View Article] [PubMed] [Google Scholar]

Harrison OB, Evans NJ, Blair JM, Grimes HS, Tinsley CR et al. Epidemiological evidence for the role of the hemoglobin receptor, hmbR, in meningococcal virulence. J Infect Dis 2009; 200:94–98 [View Article] [PubMed] [Google Scholar]

Deghmane A-E, Haeghebaert S, Hong E, Jousset A, Barret A-S et al. Emergence of new genetic lineage, ST-9316, of Neisseria meningitidis group W in Hauts-de-France region, France 2013-2018. J Infect 2020; 80:519–526 [View Article] [PubMed] [Google Scholar]

Clemence MEA, Maiden MCJ, Harrison OB. Characterization of capsule genes in non-pathogenic Neisseria species. Microb Genom 2018; 4:e000208 [View Article] [PubMed] [Google Scholar]

Kenyon CR, Schwartz IS. Effects of sexual network connectivity and antimicrobial drug use on antimicrobial resistance in Neisseria gonorrhoeae. Emerg Infect Dis 2018; 24:1195–1203 [View Article] [Google Scholar]

Gaspari V, Djusse ME, Morselli S, Rapparini L, Foschi C et al. Non-pathogenic Neisseria species of the oropharynx as a reservoir of antimicrobial resistance: a cross-sectional study. Front Cell Infect Microbiol 2023; 13:1–8 [View Article] [PubMed] [Google Scholar]

Dong HV, Pham LQ, Nguyen HT, Nguyen MXB, Nguyen TV et al. Decreased cephalosporin susceptibility of oropharyngeal Neisseria species in antibiotic-using men who have sex with men in Hanoi, Vietnam. Clin Infect Dis 2020; 70:1169–1175 [View Article] [PubMed] [Google Scholar]

Nakayama SI, Shimuta K, Furubayashi K-I, Kawahata T, Unemo M et al. New ceftriaxone- and multidrug-resistant Neisseria gonorrhoeae strain with a novel mosaic penA gene isolated in Japan. Antimicrob Agents Chemother 2016; 60:4339–4341 [View Article] [PubMed] [Google Scholar]

Sánchez-Busó L, Cole MJ, Spiteri G, Day M, Jacobsson S et al. Europe-wide expansion and eradication of multidrug-resistant Neisseria gonorrhoeae lineages: a genomic surveillance study. Lancet Microbe 2022; 3:e452–e463 [View Article] [PubMed] [Google Scholar]